

Two-dimensional correlation propagation dynamics with a cluster discrete phase-space method

Kazuma Nagao^{1,2,*} and Seiji Yunoki^{1,2,3,4}

¹*Computational Materials Science Research Team,
RIKEN Center for Computational Science (R-CCS), Hyogo 650-0047, Japan*

²*Quantum Computational Science Research Team,
RIKEN Center for Quantum Computing (RQC), Wako, Saitama 351-0198, Japan*

³*Computational Condensed Matter Physics Laboratory,
RIKEN Cluster for Pioneering Research (CPR), Saitama 351-0198, Japan*

⁴*Computational Quantum Matter Research Team,
RIKEN Center for Emergent Matter Science (CEMS), Saitama 351-0198, Japan*

(Dated: May 9, 2024)

Nonequilibrium dynamics of highly-controlled quantum systems is a challenging issue in statistical physics and quantum many-body physics, relevant to recent experimental developments of analog and digital quantum simulations. In this work, we develop a discrete phase-space approach for general $SU(N)$ spin systems that utilizes cluster mean field equations, which capture non-trivial quantum correlations inside each cluster, beyond the capability of the standard discrete truncated Wigner approximation for individual classical spins. Our formalism, based on a cluster phase-point operator, makes it possible to realize scalable numerical samplings of cluster phase-space variables, where the total number of noise variables for a direct product state is independent of the choice of the separation into finite regions of clusters. We numerically demonstrate that the cluster discrete truncated Wigner approximation (C-dTWA) method can reproduce key results in a recent experiment on the correlation propagation dynamics in a two dimensional Bose-Hubbard system. We also compare the results of C-dTWA for clusters of 2×2 sites with those of a two-dimensional tensor network method and discuss that both approaches agree very well in a short time region, where the energy is well conserved in the tensor network simulations. Since we formulate the C-dTWA method in a general form, it can be potentially applied to various dynamical problems in isolated and open quantum systems even in higher dimensions.

I. INTRODUCTION

Recent experimental advances of analog and digital quantum simulations have stimulated exploration of nonequilibrium quantum dynamics of strongly interacting systems. Typical experimental systems, where the real time quantum evolution is accessible in a highly controlled manner, include ultracold atoms and molecules in optical lattices [1–4], trapped ions [5, 6], optical tweezer arrays loaded with Rydberg atoms [7–10], and superconducting qubits [11, 12]. These platforms have been exploited to realize various types of quantum dynamics, e.g., quantum thermalization [1, 13, 14], nonergodic dynamics in many-body localization (MBL) regimes [15–17], correlation propagation dynamics after quenches [18, 19], discrete time crystalline states [20–22], and superdiffusive magnetization dynamics in a quantum circuit [23].

Quantitative numerical methods are highly imperative for advancing experimental techniques for controlling quantum dynamics and for testing the foundation of nonequilibrium statistical mechanics with the cross-check against quantum simulation results. Nevertheless, simulating quantum dynamics on classical computers typically suffers from unavoidable properties in many-body systems, such as the exponential increase of Hilbert space

dimension and the sign problem in continuous time quantum Monte Carlo methods. The tensor network method provides a versatile framework to reduce the computational cost in simulating coherent quantum dynamics [24–28]. Regardless of many advantages in the tensor network method, its efficient application is typically restricted to low-entangled states in one-dimensional short-range interacting systems. The phase space method offers another approach to analyze quantum dynamics of many-body systems in a semiclassical manner [29, 30]. Among many approaches utilizing different representations, such as the positive- P representation [31–33] and the Wigner-Weyl-Moyal representation [30, 34–39], the discrete truncated Wigner approximation (dTWA) is a valuable scheme [3, 40–47], since it gives a natural semiclassical expression of finite-dimensional systems comprised of $SU(N)$ group operators.

The dTWA is formulated only in terms of site-decoupled mean-field dynamics of spin variables, whose initial conditions are stochastically taken from a positive probability distribution without Gaussian approximation. Therefore, the computational cost is still polynomial in the increase of system size or particle number. However, the accuracy is, in general, limited to a short time regime because of the ignorance of higher order quantum effects truncated in such a leading order description. The performance evaluations for $N = 2$ have been discussed for typical spin-1/2 models in

* kazuma.nagao@riken.jp

Refs. [44, 48]. Additionally, in Ref. [49], the first author of this paper and others have attempted to apply the SU(3) dTWA and the Gaussian SU(3) TWA to a quantum quench experiment on single-particle correlations in a two-dimensional strongly interacting Bose-Hubbard system [19]. However, it has been argued that the results from these approaches show noticeable deviations from the experimental results even at quite short times.

Extension beyond the capability of the single-site dTWA has been explored in previous studies [44, 50, 51], which is based on extended mean-field theory exploiting the Bogoliubov-Born-Green-Kirkwood-Yvon (BBGKY) hierarchy truncation. However, this approach suffers from numerical instabilities in the time evolution [44]. There is another idea beyond the single site description for spins, namely the cluster truncated Wigner approximation (CTWA) [52]. This approach introduces cluster operators, each of which envelops multiple Pauli operators over a finite region of real space, in order to improve the accuracy of semiclassical approximation. Nevertheless, the sampling of cluster variables suffers from several problems. For instance, a classical SU(N) spin representation of the CTWA exploits a Gaussian approximation for the exact Wigner function. Since the total number of Gaussian noise variables increases with the dimension of possible states in a cluster, the computational difficulty increases with the cluster size [52]. Moreover, the construction of Gaussian Wigner functions is typically very complicated and hard to generalize to various situations, preventing wide applications of this promising method. Therefore, it is highly desirable to develop an approach that can diminish such difficulties in the numerical sampling by utilizing techniques in the dTWA.

In this paper, we present a general framework to combine the CTWA approach and the sampling technique in the SU(N) dTWA. We call our strategy the cluster discrete TWA (C-dTWA). Our formulation is constructed in terms of *dynamical cluster phase-point operators*, which are defined for an arbitrary set of clusters. An advantage of this is that one can realize scalable numerical samplings for fluctuating cluster variables with positive definite probabilities. The scalability is due to the fact that the total number of initial fluctuations is independent of the size of clusters, but only depends on the total system size. Therefore, the numerical sampling is easy to scale regardless of the particular choice of clustering. We specifically apply the C-dTWA to the correlation propagation dynamics in a two-dimensional Bose-Hubbard system [19, 49, 53] and demonstrate that the method successfully improves the accuracy of the previous SU(3) dTWA. In addition, we evaluate the performance of C-dTWA in comparison with experimental results in Ref. [19] and the corresponding tensor-network results, the latter being based on the infinite projected entangled pair states (iPEPS) method [53].

The rest of this paper is organized as follows. In Sec. II, we formulate the C-dTWA for a generic system comprised of SU(N) spins. In Sec. III, we present an ap-

plication of the method to a strongly interacting Bose-Hubbard system and demonstrate the performance of C-dTWA in comparison with the experiment and other numerical methods. In Sec. IV, we conclude the paper with the future perspective. In Appendix A, additional results are provided to compare the C-dTWA and Gaussian CTWA methods.

II. FORMULATION: CLUSTER-DTWA FOR SU(N) SPIN SYSTEMS

For concreteness, we specifically consider a generic SU(N) spin system isolated from the environment described by the following Hamiltonian:

$$\hat{\mathcal{H}} = \sum_{i,j,a,b} J_{i,j}^{a,b} \hat{s}_i^a \hat{s}_j^b + \sum_{i,a} h_i^a \hat{s}_i^a, \quad (1)$$

where i and j are site indices in real space, and a and b are internal indices on the spin space. The spin commutators $[\hat{s}_j^a, \hat{s}_j^b] = i \sum_{c=1}^N \epsilon_{abc} \hat{s}_j^c \delta_{j,j'}$ determine the dynamics of quantum states. The spin operators \hat{s}_j^a are Hermite and traceless, i.e., $(\hat{s}_j^a)^\dagger = \hat{s}_j^a$ and $\text{Tr} \hat{s}_j^a = 0$. For later use, we introduce $V = \{1, 2, \dots, N_s\}$, where N_s is the total number of sites.

Let us define clusters of individual SU(N) spins as illustrated in Fig. 1. A key ingredient in our formulation is a cluster phase-point operator $\hat{\mathcal{A}}_{S_\mu} = \hat{A}_{j_1} \otimes \hat{A}_{j_2} \cdots \otimes \hat{A}_{j_l} \in \mathcal{H}^{\otimes l}$ on a finite region S_μ , where μ is the label of the cluster, $\{j_1, j_2, \dots, j_l\} = S_\mu$, and $l = \dim(S_\mu)$ is the size of the cluster. It gives a phase-space representation of the time-dependent density matrix operator $\hat{\rho}(t) = \hat{U}(t, 0) \hat{\rho}(t=0) \hat{U}^\dagger(t, 0)$, i.e.,

$$\hat{\rho}(t) = \hat{U}(t, 0) \left(\overline{\bigotimes_{\mu \in V_c} \hat{\mathcal{A}}_{S_\mu}} \right) \hat{U}^\dagger(t, 0), \quad (2)$$

where V_c is the set of indices to enumerate clusters. In the single-site dTWA, $V_c = V$ holds. In this work, we assume that $\hat{\rho}(t=0)$ is a factorized operator over clusters, e.g., a direct product pure state. The overline indicates an ensemble average over different configurations of on-site classical spins $r_i^a \in \mathbb{R}$. The direct sum of S_μ covers V , i.e., $\cup_{\mu \in V_c} S_\mu = V$. The onsite operator \hat{A}_j is expanded such that $\hat{A}_j = N^{-1} \hat{\mathbb{1}}_j + g^{-1} \sum_a r_i^a \hat{s}_i^a$, where $g = \text{Tr}(\hat{s}_i^a)^2$ is a normalization factor. The fluctuations of r_i^a are distributed according to a set of positive probabilities made in a quantum-state-tomography method for SU(N) systems. It is a generalization of the state-of-the-art sampling method in the generalized dTWA (GDTWA) [42]. Hence, $\hat{\rho}(t=0)$ is reconstructed as the average of *measurement outcomes of local spin configurations*.

Next, we approximate the time evolution of $\hat{\rho}(t)$ in a numerically tractable manner. Within the dTWA for the cluster representation, the density matrix operator at time t becomes $\hat{\rho}(t) \approx \overline{\bigotimes_{\mu \in V_c} \hat{\mathcal{A}}_{S_\mu}^{\text{cl}}(t)}$. The cluster

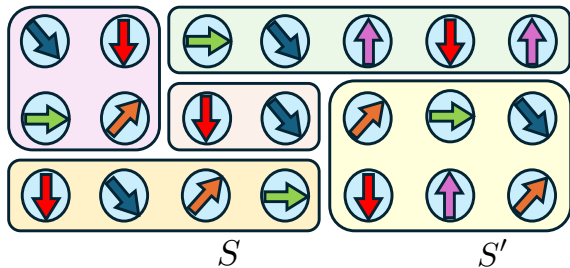


FIG. 1. Clustering a $SU(N)$ spin system with a set of finite regions. The regions, such as S and S' , are introduced to define cluster operators enveloping individual spins. In the C-dTWA, each region has its time-dependent cluster phase-point operator evolving according to a cluster mean-field equation.

phase-point operators $\hat{\mathcal{A}}_{S_\mu}^{\text{cl}}(t)$ are updated, step by step, according to a cluster mean-field equation, i.e.,

$$\hbar \partial_t \hat{\mathcal{A}}_{S_\mu}^{\text{cl}}(t) = -i[\hat{\Gamma}_{S_\mu}^{\text{intra}} + \hat{\Phi}_{S_\mu}^{\text{inter}}, \hat{\mathcal{A}}_{S_\mu}^{\text{cl}}(t)]. \quad (3)$$

For the Hamiltonian operator in Eq. (1), intra-cluster correlations inside each cluster are described by $\hat{\Gamma}_{S_\mu}^{\text{intra}} = \sum_{i \in S_\mu} \sum_a h_i^a \hat{s}_i^a + \sum_{i,j \in S_\mu} \sum_{a,b} J_{i,j}^{a,b} \hat{s}_i^a \hat{s}_j^b$. On the other hand, inter-cluster couplings reduce to $\hat{\Phi}_{S_\mu}^{\text{inter}} = \sum_{i \in S_\mu} \sum_{\nu \neq \mu} \sum_{j \in S_\nu} \sum_{a,b} J_{i,j}^{a,b} \hat{s}_i^a \langle \hat{s}_j^b \rangle_{S_\nu}$. In this contribution, $\langle \hat{s}_j^b \rangle_{S_\nu} = \text{Tr} [\hat{s}_j^b \hat{\mathcal{A}}_{S_\nu}^{\text{cl}}(t)]$ are regarded as *cluster mean fields* coupled to the cluster on S_μ .

In numerical simulations, the state of $\hat{\mathcal{A}}_{S_\mu}^{\text{cl}}(t)$ is registered as a set of finite dimensional matrices. Drawing a random set of r_i^a over the whole system, $\bigotimes_{\mu \in \mathcal{V}_c} \hat{\mathcal{A}}_{S_\mu}^{\text{cl}}(t)$ is an N^{N_s} dimensional random matrix, whose ensemble average is no longer a direct product matrix for $t > 0$. This property reflects the dynamical growth of inter correlations between clusters [44, 52]. The intra cluster correlations are exactly incorporated along the trajectory dynamics beyond the capability of the single-site dTWA. The benefit of the sampling method is that the total number of random numbers, i.e., r_i^a , is independent of the choice of clusters. This point can be contrasted with the cases of CTWA. Indeed, a Gaussian Wigner function, even as simplified with a dimensional reduction technique for an appropriate operator basis of clusters, includes $2D$ fluctuating real variables, where D is the cluster size [52]. Hence, the total number of variables increases with D , and it becomes significantly large for $D \gg 1$. In Appendix A, we numerically show that the C-dTWA can reproduce the same results as those obtained by the CTWA for a $SU(2)$ transverse Ising model, implying the consistency and an advantage of the C-dTWA method.

III. CORRELATION PROPAGATION DYNAMICS IN TWO DIMENSIONS

To demonstrate the power of exploiting correlated clusters in dTWA, we specifically analyze the correlation propagation dynamics in the isolated Bose-Hubbard model on a square lattice [19, 53]. The Hamiltonian is given by

$$\hat{H} = -J \sum_{\langle i,j \rangle} (\hat{a}_i^\dagger \hat{a}_j + \text{H.c.}) + \frac{U}{2} \sum_i \hat{a}_i^\dagger \hat{a}_i^\dagger \hat{a}_i \hat{a}_i, \quad (4)$$

where the hopping amplitude J and the onsite interaction U are tunable via the isotropic lattice depth \mathcal{V} . In the quench experiment, the dynamics is measured in a strongly interacting regime satisfying $U \gg J$. In that regime, the relevant Hilbert space is restricted. Here, the maximum occupation is set to $n_{\text{max}} = 2$. Then, an arbitrary local operator can be represented in terms of a three-dimensional matrix, which can be decomposed in base matrices in the $SU(3)$ group [35, 49]. The state truncation leads to a model of interacting $SU(3)$ pseudospins from the original Hamiltonian, which is a specific case of the general model in Eq. (1).

We analyze a quantum quench starting from a direct product state. The relevant quantity is the equal-time single-particle correlation function $C_{(\Delta_x, \Delta_y)}^{\text{sp}}(t) = N_s^{-1} \sum_{i,j} \langle \hat{a}_i^\dagger(t) \hat{a}_j(t) \rangle$, where $\sum_{i,j}$ indicates the summation with the conditions $|x_i - x_j| = \Delta_x$ and $|y_i - y_j| = \Delta_y$ [49], and (x_i, y_i) represents the coordinate of site i . The propagation of correlations is measured in the units of the Euclidean distance $|\mathbf{r}| = \sqrt{\Delta_x^2 + \Delta_y^2}$. Before a quench, the system is prepared in the ground state of the system at $U = \infty$, which is the unit filling Mott insulating state $|\psi_{\text{ini}}\rangle = \prod_{i=1}^{N_s} |1\rangle_i$. Then, the optical lattice depth $s = \mathcal{V}/E_R$ is linearly varied for a finite ramp time τ_Q , where E_R is the recoil energy of the system. The time sequence is a ramp-down of the lattice, i.e., $s(t) = \frac{t+\tau_Q}{\tau_Q}(s_f - s_i) + s_i$, where $s_f = 9$ and $s_i = 15$. In particular, the final lattice depth implies $U/J = 19.6$. The ramp time is sufficiently quick as $\tau_Q = 0.1\text{ms}$ [49, 53]. For the following analyses, we assume periodic boundary conditions and the lattice geometry has totally $N_s = L_x \times L_y = 400$ sites with $L_x = L_y = 20$.

In Fig. 2, we monitor the dynamics of single-particle correlation functions for $|\mathbf{r}| = 1, \sqrt{2}, 2$, and 3 within the C-dTWA with clusters of 2×2 sites in comparison with the results from the iPEPS [53], the $SU(3)$ dTWA, and the experiment [19]. Note that the sampling scheme for the $SU(3)$ dTWA is a quantum-state-tomography method in the GDTWA [42, 49]. The illustration of this clustering is shown in Fig. 3. Figure 2(a) shows the results for the nearest-neighbor correlation $C_{|\mathbf{r}|=1}^{\text{sp}} = (C_{(1,0)}^{\text{sp}} + C_{(0,1)}^{\text{sp}})/2$, where the first peak appears around at $t \sim 0.12\hbar/J_{\text{fin}}$ in the results of the iPEPS, the C-dTWA, and the experiment. The results

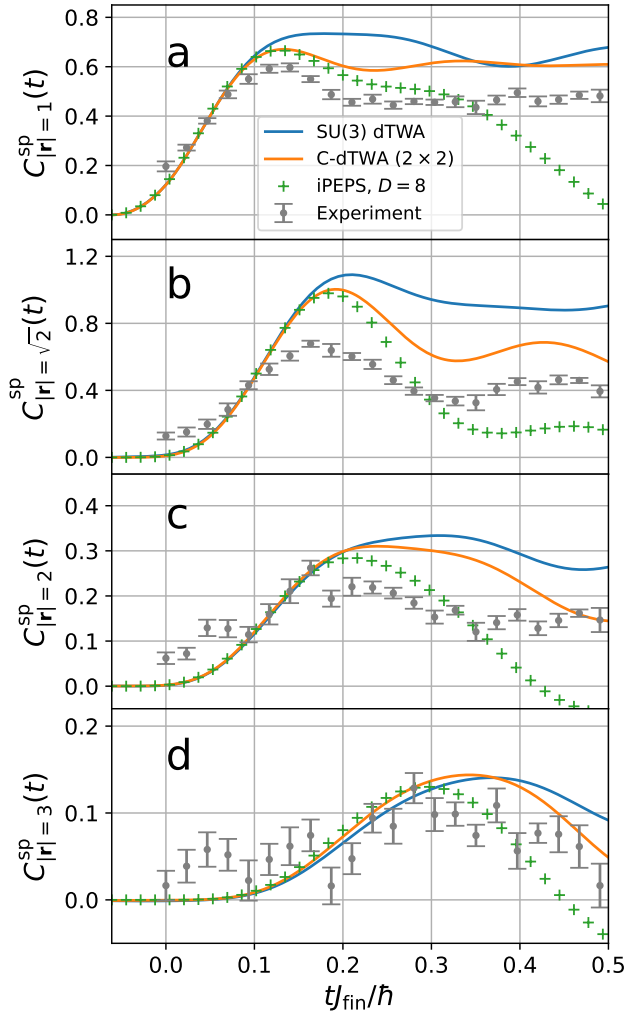


FIG. 2. Time evolution of the single-particle correlation functions $C_{|\mathbf{r}|}^{\text{sp}}(t)$ after a finite speed ramp down of the optical lattice depth ($t = 0$) at distances (a) $|\mathbf{r}| = 1$, (b) $|\mathbf{r}| = \sqrt{2}$, (c) $|\mathbf{r}| = 2$, and (d) $|\mathbf{r}| = 3$ evaluated by the C-dTWA with clusters of 2×2 sites (orange line) and the SU(3) dTWA (blue line). The total number of sites is $N_s = 400$ with $L_x = L_y = 20$ under periodic boundary conditions. For comparison, the results for the iPEPS with the bond dimension $D = 8$ (green crosses) [53] and the experiments (gray points with error bars) [19] are also plotted.

of the C-dTWA and the iPEPS are in good agreement for $t \lesssim 0.2\hbar/J_{\text{fin}}$. The peak times are consistent with that of the experimental data. However, the SU(3) dTWA cannot exhibit such a peak because of the breakdown of the method for $t \gtrsim 0.1\hbar/J_{\text{fin}}$, as also discussed in the previous work [49]. In the iPEPS calculations, the energy is approximately conserved for $t \lesssim 0.4\hbar/J_{\text{fin}}$ [53]. Even at longer times for $t \gtrsim 0.4\hbar/J_{\text{fin}}$, where the iPEPS is no longer validated, the result of the C-dTWA is qualitatively similar to the behavior of the experiment data.

Figure 2(b) shows the results for $C_{|\mathbf{r}|=\sqrt{2}}^{\text{sp}} = C_{(1,1)}^{\text{sp}}$. The values of these correlation functions in the C-dTWA and

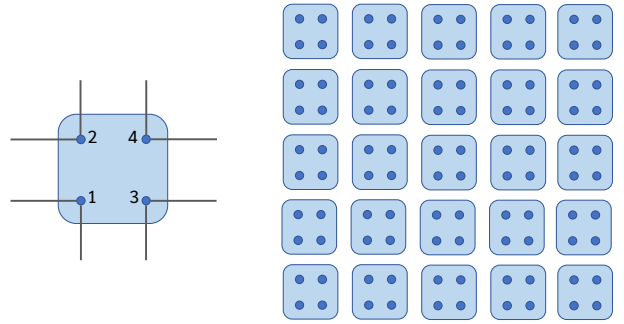


FIG. 3. Cluster phase-space representation of the two-dimensional Bose-Hubbard system with clusters of 2×2 sites. The index rule inside a cluster is given in the left object with outer eight legs, representing nonlinear couplings to the other clusters.

the iPEPS also agree very well for $t \lesssim 0.2\hbar/J_{\text{fin}}$. Moreover, the first peak times of the correlation functions are consistent with that for the experiment. However, the corresponding peak in the SU(3) dTWA is slightly shifted at later times. Besides this, the C-dTWA also produces the second peak at $t \sim 0.43\hbar/J_{\text{fin}}$, which is qualitatively consistent with the experimental data. Furthermore, Figs. 2(c) and 2(d), showing the results for the correlation functions with $|\mathbf{r}| = 2$ and 3, respectively, demonstrate that the intra cluster fluctuations treated within the C-dTWA, which may still be less estimated, lead to improvement of the first peak times over the SU(3) dTWA, by comparing the results with those of the iPEPS and the experiment. However, there are deviations of the peak times between the C-dTWA and iPEPS results. To confirm the origin of this deviation comprehensively, it is necessary to incorporate larger clusters in the simulations, which is beyond the scope of this study with the available computational resource, thus left for a future study.

To gain insights on the quantitative limitation of the C-dTWA, we compare the semiclassical dynamics obtained by the C-dTWA with the corresponding exact ones for a small system composed of $N_s = 4 \times 4 = 16$ sites. As in the previous case, the initial state is set to be the unit filling Mott insulating state. For simplicity, here we assume $\tau_Q = 0$, implying a sudden quench from $U/J = \infty$ to $U/J = 19.6$. Figure 4 shows the results for the single-particle correlation functions at $|\mathbf{r}| = 1$ and $\sqrt{2}$ calculated by the C-dTWA with clusters of 2×2 sites. The C-dTWA method can indeed capture the first peaks at the early times. However, for $|\mathbf{r}| = 1$ ($|\mathbf{r}| = \sqrt{2}$), the deviations from the exact results are noticeable for $t \gtrsim 0.25\hbar/J$ ($t \gtrsim 0.35\hbar/J$). This is attributed to the higher order contributions that are relevant to the long time quantum dynamics.

These comparisons demonstrate that intra-cluster correlations are essential for describing the important features in the propagation dynamics, such as the first peak

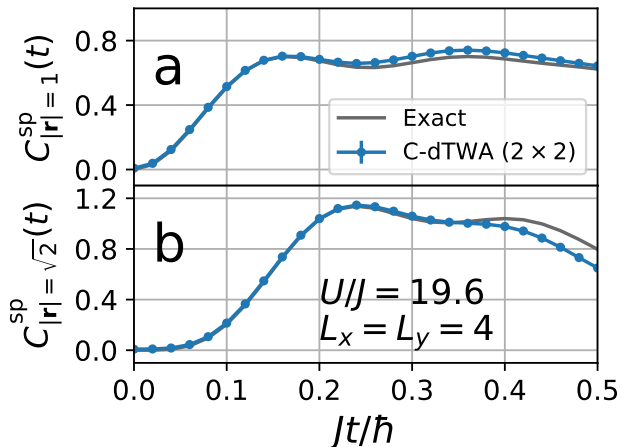


FIG. 4. Time evolution of the single-particle correlation functions $C_{|\mathbf{r}|}^{\text{sp}}(t)$ at distances (a) $|\mathbf{r}| = 1$ and (b) $|\mathbf{r}| = \sqrt{2}$ after a sudden quench at $t = 0$ for $N_s = 16$ with $L_x = L_y = 4$ under periodic boundary conditions. The initial state is set to be the unit filling Mott insulating state and the final state of the sudden quench implies $U/J = 19.6$. For comparison, the exact results obtained by using QuSpin library [54, 55] are also plotted by solid curves.

times, and the qualitative behavior after the first peaks. Nevertheless, as shown in Fig. 4 in the comparison with the numerically exact results, the C-dTWA method with clusters up to 2×2 sites fails to fully capture quantum dynamics, particularly after the early time stage. In principle, the C-dTWA method becomes asymptotically exact with increasing the cluster size to the total system size. However, in practice, the cluster size employed is strictly limited by available computational resources. In future studies, we will develop a nontrivial parallelization approach along with a data compression technique to increase the maximum size of clusters by exploiting a modern large-scale supercomputer system.

IV. CONCLUSIONS

In conclusions, we have combined the cluster phase space representation method and the discrete truncated Wigner sampling method for finite-dimensional $SU(N)$ spin systems. To demonstrate the power of the method, we have applied the C-dTWA method to the correlation spreading dynamics in a two-dimensional Bose-Hubbard model. The results of the C-dTWA with clusters of 2×2 sites agree with those of the iPEPS calculations at short times where the energy conservation in the iPEPS calculations is satisfied. Even at longer times, the C-dTWA can reproduce the qualitative behavior of the experimental results, which is not captured in the iPEPS calculations.

Although our study in this paper focuses mainly on the performance of the method, the C-dTWA method paves the way to exploring nontrivial dynamics beyond

the current capability of other numerical methods such as tensor network methods and the single-site dTWA. For instance, our method can evaluate long-distance correlations, which are difficult to treat in the iPEPS approach. This would be important in extracting a propagation velocity from the dynamics of correlation functions, which provides a better estimation of the Lieb-Robinson bound on the quantum information propagation. Moreover, the cluster phase-point operator formalism developed here for individual $SU(N)$ spins is versatile because it can be readily and directly generalized to open quantum systems described by the Lindblad master equation [56]. These potential applications will be investigated elsewhere.

Note added— During completing this paper, we were aware of a recent related study on a cluster generalization of the generalized discrete truncated Wigner approximation (GDTWA) [57]. Although the concept is similar in the spirit of formulation, we notice differences in the following points. First, our formulation is based on a cluster phase-point operator, which is valuable for practical calculations, while their approach is a simple generalization of the GDTWA for $SU(N)$ systems. Second, their main application focuses on an experiment of spin-3 chromium atoms in a three-dimensional optical lattice, where a neighboring pair of $s = 3$ spins is regarded as a $SU(49)$ spin system. In our study, we discuss an application to a two-dimensional Bose-Hubbard system, where we treat a subsystem with 2×2 sites as a $SU(81)$ spin system.

ACKNOWLEDGMENTS

We thank Ryui Kaneko, Rongyang Sun, and Ipeei Danshita for fruitful discussions. We also thank Yosuke Takasu and Yoshiro Takahashi for providing experimental data in Ref. [19]. This work is based on results obtained in part from a project, JPNP20017, subsidised by the New Energy and Industrial Technology Development Organization (NEDO), Japan. We acknowledge the support from JSPS KAKENHI (Grant No. JP21H04446) from the Ministry of Education, Culture, Sports, Science and Technology (MEXT), Japan. We also appreciate the funding received from JST COINNEXT (Grant No. JPMJPF2221) and the Program for Promoting Research of the Supercomputer Fugaku (Grant No. MXP1020230411) from MEXT, Japan. Furthermore, we acknowledge the support from the RIKEN TRIP project and the COE research grant in computational science from Hyogo Prefecture and Kobe City through the Foundation for Computational Science. The truncated Wigner simulations have been carried out on the HOKUSAI supercomputing system at RIKEN and the supercomputer Fugaku provided by the RIKEN Center for Computational Science. The numerically exact calculations have been done using iTensor [58] and QuSpin [54, 55] packages.

Appendix A: Revisit to a four site transverse-field Ising chain

In this appendix, we revisit the benchmark of the cluster phase space description, which was also discussed in Ref. [52], for a system of four coupled Pauli spins described by the following Hamiltonian:

$$\hat{H}_{\text{Ising}} = J \sum_{i=1}^3 \hat{\sigma}_z^{(i)} \hat{\sigma}_z^{(i+1)} + h_x \sum_{i=1}^4 \hat{\sigma}_x^{(i)}. \quad (\text{A1})$$

Here, $\hat{\sigma}_\gamma^{(i)}$ is the γ component of Pauli matrices with $\gamma = x, y$, and z at site i . To implement the C-dTWA, we separate the system into two subsystems and define a global phase-point operator as $\hat{A}_{\text{tot}} = \hat{A}_L \otimes \hat{A}_R$. The left and right cluster phase-point operators \hat{A}_L and \hat{A}_R are decomposed respectively as

$$\hat{A}_L = \frac{1}{2^2} \sum_{m,n \in \{0,x,y,z\}} X_{m,n}^{(1,2)} \hat{\sigma}_m^{(1)} \otimes \hat{\sigma}_n^{(2)} \quad (\text{A2})$$

and

$$\hat{A}_R = \frac{1}{2^2} \sum_{m,n \in \{0,x,y,z\}} X_{m,n}^{(3,4)} \hat{\sigma}_m^{(3)} \otimes \hat{\sigma}_n^{(4)}, \quad (\text{A3})$$

where $\hat{\sigma}_0^{(i)}$ is the identity matrix and $X_{0,0}^{(1,2)} = X_{0,0}^{(3,4)} = 1$ because the dynamics is unitary.

Since inter-site correlations factorize in a direct product state, we impose the initial conditions on the cluster variables at $t = 0$ as

$$X_{m,n}^{(i,j)}(t=0) = \zeta_m^{(i)} \zeta_n^{(j)}, \quad (\text{A4})$$

where $\zeta_m^{(i)}$ describe onsite spin fluctuations. For $|\uparrow\rangle$ or $|\downarrow\rangle$, the x and y components $\zeta_x^{(i)}$ and $\zeta_y^{(i)}$ take $+1$ or -1 randomly with an equal probability $1/2$, while the z components stay constant. Figure 5 shows the results for the quench dynamics of $M_z = \sum_{i=1}^4 (-1)^{i-1} \langle \hat{\sigma}_z^{(i)}(t) \rangle$, starting from the initial state $|\psi(t=0)\rangle = |\uparrow, \downarrow, \uparrow, \downarrow\rangle$. In this figure, we compare the C-dTWA results with the Gaussian CTWA results in Ref. [52] and find that these results are in excellent agreement. Note that for fair comparison, the number of trajectories is 20000 in both methods.

The Gaussian Wigner function W_{Gauss} for the product state $|\uparrow, \downarrow, \uparrow, \downarrow\rangle$ has a product form, i.e., $W_{\text{Gauss}} = W_L W_R$. Following the construction described in

Ref. [52], the distribution $W_{L(R)}$ on each cluster is found to be

$$\begin{aligned} W_{L(R)} = & \frac{1}{\mathcal{Z}} \delta(x_{15} + 1) \delta(x_3 + 1) \delta(x_{12} - 1) \\ & \times \delta(x_1 - x_{13}) \delta(x_2 - x_{14}) \delta(x_5 - x_{10}) \\ & \times \delta(x_4 + x_7) \delta(x_6 + x_9) \delta(x_8 + x_{11}) \\ & \times e^{-\frac{1}{2} \sum_{\alpha \in \{1,2,4,5,6,8\}} x_\alpha^2}, \end{aligned} \quad (\text{A5})$$

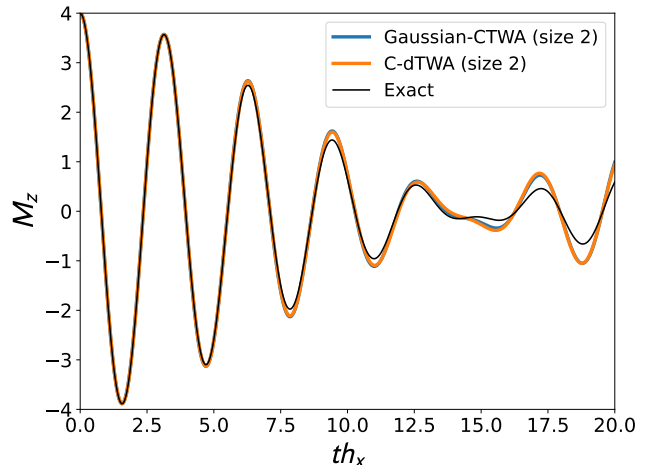


FIG. 5. Time evolution of the magnetization M_z for the four site Ising chain evaluated using the C-dTWA with clusters of 2 sites (orange) and the Gaussian CTWA (blue). Here, we set $J = 1/8$ and $h_x = 1$, the same values used in Ref. [52]. For comparison, the exact results (obtained by iTensor [58]) are also plotted by black. Note that the orange and blue curves are essentially identical in this scale.

where \mathcal{Z} is the normalization factor. The basis operators on the clusters are defined as

$$\begin{aligned} \hat{X}_1 &= \hat{\sigma}_0 \otimes \hat{\sigma}_x, & \hat{X}_2 &= \hat{\sigma}_0 \otimes \hat{\sigma}_y, & \hat{X}_3 &= \hat{\sigma}_0 \otimes \hat{\sigma}_z, \\ \hat{X}_4 &= \hat{\sigma}_x \otimes \hat{\sigma}_0, & \hat{X}_5 &= \hat{\sigma}_x \otimes \hat{\sigma}_x, & \hat{X}_6 &= \hat{\sigma}_x \otimes \hat{\sigma}_y, \\ \hat{X}_7 &= \hat{\sigma}_x \otimes \hat{\sigma}_z, & \hat{X}_8 &= \hat{\sigma}_y \otimes \hat{\sigma}_0, & \hat{X}_9 &= \hat{\sigma}_y \otimes \hat{\sigma}_x, \\ \hat{X}_{10} &= \hat{\sigma}_y \otimes \hat{\sigma}_y, & \hat{X}_{11} &= \hat{\sigma}_y \otimes \hat{\sigma}_z, & \hat{X}_{12} &= \hat{\sigma}_z \otimes \hat{\sigma}_0, \\ \hat{X}_{13} &= \hat{\sigma}_z \otimes \hat{\sigma}_x, & \hat{X}_{14} &= \hat{\sigma}_z \otimes \hat{\sigma}_y, & \hat{X}_{15} &= \hat{\sigma}_z \otimes \hat{\sigma}_z. \end{aligned}$$

The distribution $W_{L(R)}$ has six independent random numbers, and thus there are totally twelve noise variables in the whole system. By contrast, the distribution in the C-dTWA has only eight noise variables in the whole system.

-
- [1] S. Trotzky, Y.-A. Chen, A. Flesch, I. P. McCulloch, U. Schollwöck, J. Eisert, and I. Bloch, *Nature physics* **8**, 325 (2012).
[2] C. Gross and I. Bloch, *Science* **357**, 995 (2017).
[3] S. Lepoutre, J. Schachenmayer, L. Gabardos, B. Zhu,

- B. Naylor, E. Maréchal, O. Gorceix, A. M. Rey, L. Vernac, and B. Laburthe-Tolra, *Nature Communications* **10**, 1714 (2019).
[4] F. Schäfer, T. Fukuhara, S. Sugawa, Y. Takasu, and Y. Takahashi, *Nature Reviews Physics* **2**, 411 (2020).

- [5] B. P. Lanyon, C. Hempel, D. Nigg, M. Müller, R. Geritsma, F. Zähringer, P. Schindler, J. T. Barreiro, M. Rambach, G. Kirchmair, *et al.*, *Science* **334**, 57 (2011).
- [6] R. Blatt and C. F. Roos, *Nature Physics* **8**, 277 (2012).
- [7] A. M. Kaufman and K.-K. Ni, *Nature Physics* **17**, 1324 (2021).
- [8] D. Bluvstein, A. Omran, H. Levine, A. Keesling, G. Semeghini, S. Ebadi, T. T. Wang, A. A. Michailidis, N. Maskara, W. W. Ho, *et al.*, *Science* **371**, 1355 (2021).
- [9] D. Bluvstein, H. Levine, G. Semeghini, T. T. Wang, S. Ebadi, M. Kalinowski, A. Keesling, N. Maskara, H. Pichler, M. Greiner, *et al.*, *Nature* **604**, 451 (2022).
- [10] V. Bharti, S. Sugawa, M. Mizoguchi, M. Kunimi, Y. Zhang, S. De Léséleuc, T. Tomita, T. Franz, M. Weidemüller, and K. Ohmori, *Physical review letters* **131**, 123201 (2023).
- [11] M. Kjaergaard, M. E. Schwartz, J. Braumüller, P. Krantz, J. I.-J. Wang, S. Gustavsson, and W. D. Oliver, *Annual Review of Condensed Matter Physics* **11**, 369 (2020).
- [12] Y. Kim, A. Eddins, S. Anand, K. X. Wei, E. Van Den Berg, S. Rosenblatt, H. Nayfeh, Y. Wu, M. Zaletel, K. Temme, *et al.*, *Nature* **618**, 500 (2023).
- [13] T. Langen, T. Gasenzer, and J. Schmiedmayer, *Journal of Statistical Mechanics: Theory and Experiment* **2016**, 064009 (2016).
- [14] A. M. Kaufman, M. E. Tai, A. Lukin, M. Rispoli, R. Schittko, P. M. Preiss, and M. Greiner, *Science* **353**, 794 (2016).
- [15] J.-y. Choi, S. Hild, J. Zeiher, P. Schauß, A. Rubio-Abadal, T. Yefsah, V. Khemani, D. A. Huse, I. Bloch, and C. Gross, *Science* **352**, 1547 (2016).
- [16] P. Bordia, H. Lüschen, S. Scherg, S. Gopalakrishnan, M. Knap, U. Schneider, and I. Bloch, *Physical Review X* **7**, 041047 (2017).
- [17] H. P. Lüschen, P. Bordia, S. S. Hodgman, M. Schreiber, S. Sarkar, A. J. Daley, M. H. Fischer, E. Altman, I. Bloch, and U. Schneider, *Physical Review X* **7**, 011034 (2017).
- [18] M. Cheneau, P. Barmettler, D. Poletti, M. Endres, P. Schauß, T. Fukuhara, C. Gross, I. Bloch, C. Kollath, and S. Kuhr, *Nature* **481**, 484 (2012).
- [19] Y. Takasu, T. Yagami, H. Asaka, Y. Fukushima, K. Nagao, S. Goto, I. Danshita, and Y. Takahashi, *Science advances* **6**, eaba9255 (2020).
- [20] J. Zhang, P. W. Hess, A. Kyprianidis, P. Becker, A. Lee, J. Smith, G. Pagano, I.-D. Potirniche, A. C. Potter, A. Vishwanath, *et al.*, *Nature* **543**, 217 (2017).
- [21] P. Frey and S. Rachel, *Science advances* **8**, eabm7652 (2022).
- [22] K. Shinjo, K. Seki, T. Shirakawa, R.-Y. Sun, and S. Yunoki, *arXiv preprint arXiv:2403.16718* (2024).
- [23] E. Rosenberg, T. Andersen, R. Samajdar, A. Petukhov, J. Hoke, D. Abanin, A. Bengtsson, I. Drozdov, C. Erickson, P. Klimov, *et al.*, *arXiv preprint arXiv:2306.09333* (2023).
- [24] U. Schollwöck, *Annals of physics* **326**, 96 (2011).
- [25] J. I. Cirac, D. Perez-Garcia, N. Schuch, and F. Verstraete, *Reviews of Modern Physics* **93**, 045003 (2021).
- [26] T. Xiang, *Density Matrix and Tensor Network Renormalization* (Cambridge University Press, 2023).
- [27] C. Mc Keever and M. Szymańska, *Physical Review X* **11**, 021035 (2021).
- [28] J. Dziarmaga and J. M. Mazur, *Physical Review B* **107**, 144510 (2023).
- [29] C. Gardiner and P. Zoller, *Quantum noise: a handbook of Markovian and non-Markovian quantum stochastic methods with applications to quantum optics* (Springer Science & Business Media, 2004).
- [30] A. Polkovnikov, *Annals of Physics* **325**, 1790 (2010).
- [31] M. J. Steel, M. Olsen, L. Plimak, P. Drummond, S. Tan, M. Collett, D. Walls, and R. Graham, *Physical Review A* **58**, 4824 (1998).
- [32] P. Deuar, A. Ferrier, M. Matuszewski, G. Orso, and M. H. Szymańska, *PRX Quantum* **2**, 010319 (2021).
- [33] P. Deuar, *Quantum* **5**, 455 (2021).
- [34] P. B. Blakie, A. Bradley, M. Davis, R. Ballagh, and C. Gardiner, *Advances in Physics* **57**, 363 (2008).
- [35] S. M. Davidson and A. Polkovnikov, *Phys. Rev. Lett.* **114**, 045701 (2015).
- [36] K. Nagao, M. Kunimi, Y. Takasu, Y. Takahashi, and I. Danshita, *Physical Review A* **99**, 023622 (2019).
- [37] K. Nagao, *Fluctuations and non-equilibrium phenomena in strongly-correlated ultracold atoms* (Springer Nature, 2020).
- [38] J. Huber, P. Kirton, and P. Rabl, *SciPost Physics* **10**, 045 (2021).
- [39] S. E. Begg, M. J. Davis, and M. T. Reeves, *Physical Review Letters* **132**, 103402 (2024).
- [40] J. Schachenmayer, A. Pikovski, and A. M. Rey, *Physical Review X* **5**, 011022 (2015).
- [41] A. P. n. Orioli, A. Signoles, H. Wildhagen, G. Günter, J. Berges, S. Whitlock, and M. Weidemüller, *Phys. Rev. Lett.* **120**, 063601 (2018).
- [42] B. Zhu, A. M. Rey, and J. Schachenmayer, *New Journal of Physics* **21**, 082001 (2019).
- [43] A. Signoles, T. Franz, R. Ferracini Alves, M. Gärttner, S. Whitlock, G. Zürn, and M. Weidemüller, *Phys. Rev. X* **11**, 011011 (2021).
- [44] M. Kunimi, K. Nagao, S. Goto, and I. Danshita, *Phys. Rev. Research* **3**, 013060 (2021).
- [45] C. D. Mink, D. Petrosyan, and M. Fleischhauer, *Phys. Rev. Research* **4**, 043136 (2022).
- [46] V. P. Singh and H. Weimer, *Physical Review Letters* **128**, 200602 (2022).
- [47] S. R. Muleady, M. Yang, S. R. White, and A. M. Rey, *Physical Review Letters* **131**, 150401 (2023).
- [48] B. Sundar, K. C. Wang, and K. R. A. Hazzard, *Phys. Rev. A* **99**, 043627 (2019).
- [49] K. Nagao, Y. Takasu, Y. Takahashi, and I. Danshita, *Phys. Rev. Res.* **3**, 043091 (2021).
- [50] L. Pucci, A. Roy, and M. Kastner, *Phys. Rev. B* **93**, 174302 (2016).
- [51] A. P. Orioli, A. Safavi-Naini, M. L. Wall, and A. M. Rey, *Physical Review A* **96**, 033607 (2017).
- [52] J. Wurtz, A. Polkovnikov, and D. Sels, *Annals of Physics* **395**, 341 (2018).
- [53] R. Kaneko and I. Danshita, *Communications Physics* **5**, 65 (2022).
- [54] P. Weinberg and M. Bukov, *SciPost Physics* **2**, 003 (2017).
- [55] P. Weinberg and M. Bukov, *SciPost Physics* **7**, 020 (2019).
- [56] K. Nagao, I. Danshita, and S. Yunoki, *arXiv preprint arXiv:2307.16170* (2023).
- [57] Y. A. Alaoui, S. R. Muleady, E. Chaparro, Y. Trifa, A. M. Rey, T. Roscilde, B. Laburthe-Tolra, and L. Vernac, *arXiv preprint arXiv:2404.10531* (2024).

- [58] M. Fishman, S. R. White, and E. M. Stoudenmire, *SciPost Phys. Codebases*, 4 (2022).